ACS NANO

www.acsnano.org

ARTICLE

Room-Temperature-Processable Wire-Templated Nanoelectrodes for Flexible and Transparent All-Wire Electronics

Sung-Yong Min,[†] Yeongjun Lee,[†] Se Hyun Kim,[‡] Cheolmin Park,[§] and Tae-Woo Lee*[,⊥]

[†]Department of Materials Science and Engineering, Pohang University of Science and Technology (POSTECH), San 31, Hyoja-dong, Nam-gu, Pohang, Gyungbuk 37673, Republic of Korea

[‡]School of Chemical Engineering, Yeungnam University, Gyeongsan, North Gyeongsang 38541, Republic of Korea

[§]Department of Materials Science and Engineering, Yonsei University, Seoul 03722, Republic of Korea

[⊥]Department of Materials Science and Engineering, Seoul National University, 1 Gwanak-ro, Gwanak-gu, Seoul 08826, Republic of Korea

Supporting Information

ABSTRACT: **Sophisticated preparation of arbitrarily long conducting nanowire electrodes on a large area is a significant requirement for development of transparent nanoelectronics. We report a position-customizable and room-temperature-processable metallic nanowire (NW) electrode array using aligned NW templates and a demonstration of transparent all-NW-based electronic applications by simple direct-printing. Well-controlled electroless-plating chemistry on a polymer NW template provided a highly conducting Au NW array with a very low resistivity of 7.5 $\mu\Omega$ cm (only 3.4 times higher than that of bulk Au), high optical transmittance (>90%), and mechanical bending stability. This method enables fabrication of all-NW-based electronic devices on various nonplanar surfaces and flexible plastic substrates. Our approach facilitates realization of advanced future electronics.**

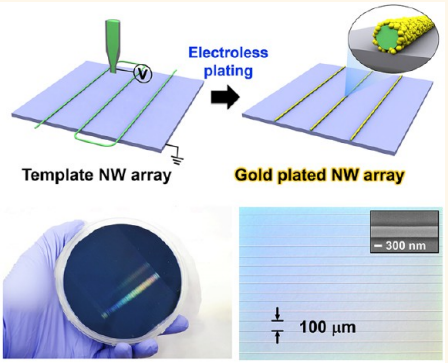

KEYWORDS: *position-customizable nanowire printing, electroless plating, transparent nanoelectrodes, metallic nanowires, all-wire electronics*

A transparent electrode is essential for realization of transparent nanoelectronic and optoelectronic devices. It must be highly conductive, transparent, and mechanically flexible for such applications. Several types of transparent electrodes have been proposed as alternatives to conventional indium tin oxide (ITO) electrodes, such as graphene, carbon nanotubes, metallic mesh, and solution-grown metallic nanowires (NWs).[1−12] Among these candidates, metallic NWs (*e.g.*, Ag NWs) are suitable as a transparent electrode owing to their simple and high-yielding preparation process and low resistivity (1.67 $\mu\Omega$ cm). However, practical applications of metallic NWs are still limited because of (i) the short NW length range from a few to tens of micrometers and (ii) randomly dispersed or entangled NW networks, which result in irregular optical and electrical characteristics and severely rough surfaces.[7,8,13−16] Therefore, development of uniform transparent electrodes on large areas requires a method to control the position and orientation of metallic NWs.

Metallic NWs with large-scale alignment can be produced using simple direct printing procedures in an individually controlled manner and used as transparent electrodes.[17−19] However, the previous printed metallic NW-based electrode requires high-temperature calcination to transform polymer/metal precursor composite NWs to metallic NWs.[17−19] This requirement hinders direct fabrication of large-scale conducting NW-based transparent electronics on flexible or stretchable substrates. To use printing technology for realization of soft electronic applications, a process for preparing highly conductive nanomaterials without high-temperature heating is required.

Here we (i) report an easy method to fabricate a position-controllable and arbitrarily long metallic NW array with high conductivity on a flexible plastic substrate without any high-temperature heating or vacuum processes and (ii) demonstrate all-NW-based transparent electronic applications including transparent transistors and heaters (Figure 1a). First, we used well-aligned organic nanowire (ONW) arrays as metallization templates. These arrays were prepared using a home-built

Received: December 6, 2016
Accepted: March 17, 2017
Published: March 17, 2017

DOI: 10.1021/acsnano.6b08172
ACS Nano 2017, 11, 3681−3689

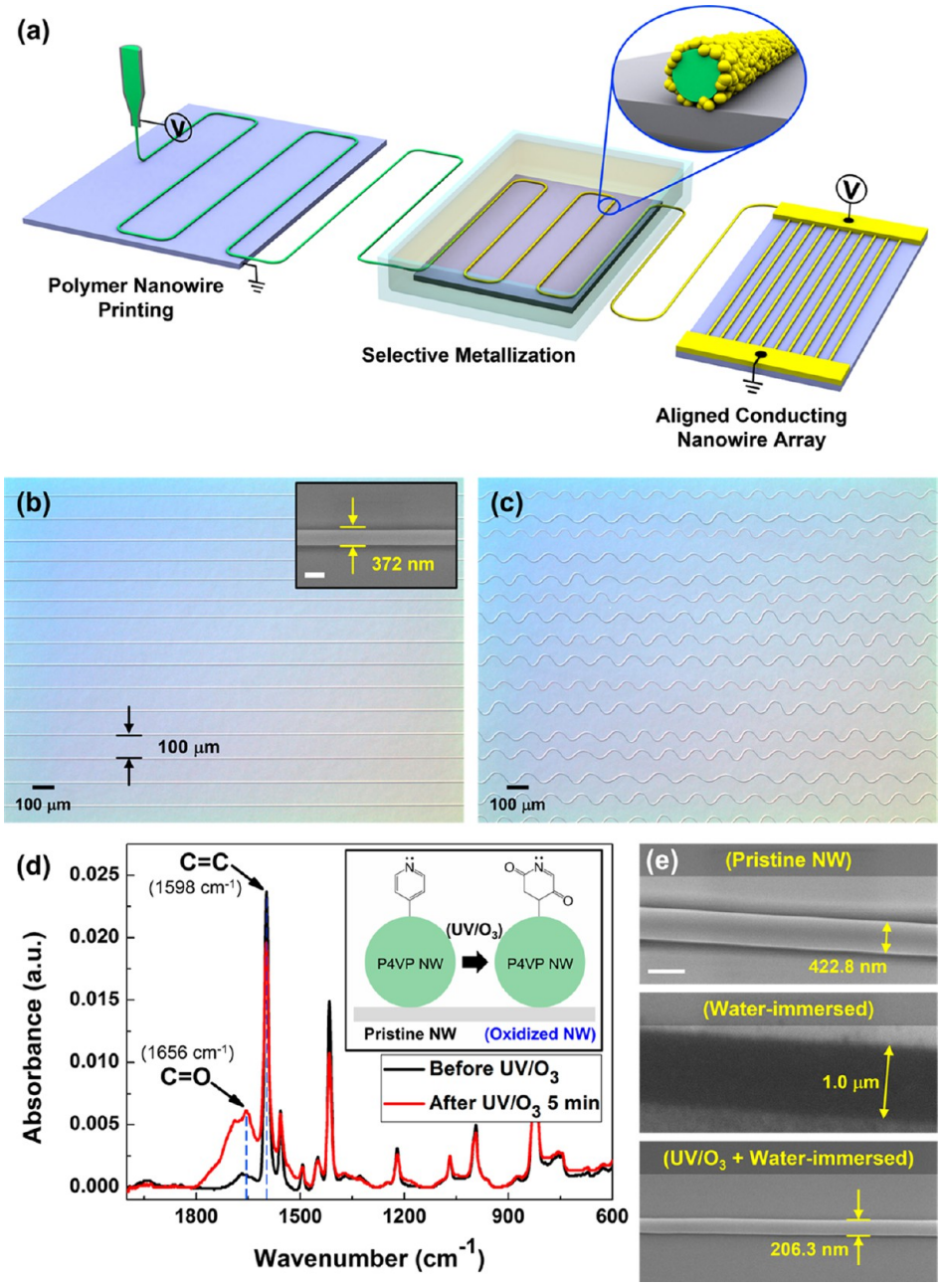

Figure 1. Preparation of a highly aligned template P4VP NW array. (a) Schematic illustration of the process to prepare a well-aligned conducting NW array. (b) Parallel and (c) wavy pattern of a printed pristine P4VP NW array with a 100 μm pitch (inset: SEM image of a P4VP NW; scale bar, 500 nm). (d) FT-IR absorbance of a P4VP NW mat before and after UV/O_3 treatment for 5 min (inset: scheme of molecular change in P4VP NW by UV/O_3 treatment). (e) SEM images of pristine P4VP NW (top) and P4VP NW after water immersion for 30 min without (center) and with UV/O_3 treatment (30 min) (bottom). Scale bar: 500 nm.

position-customizable nanowire printing (PCNP) system that can print ONWs rapidly in desired positions and orientations.[20,21] Then, by electroless plating a metal layer on the surface of printed ONWs, a core−sheath structured conducting NW array with a high optical transmittance of >90% and flexibility was attained; it also showed good electrical conductivity (average resistivity of 7.5 $\mu\Omega$ cm) without any heating or vacuum process; this resistivity is of the same order of magnitude as that of bulk Au (2.21 $\mu\Omega$ cm). We also demonstrated highly transparent and flexible all-wire electronics. Using the individually position-customizable metallic NWs and semiconducting ONWs, we prepared a direct-printed transparent all-nanowire-based transistor array with low operation voltage (<4 V) and a transparent heater with good exothermic properties.

RESULTS AND DISCUSSION

A highly aligned poly(4-vinylpyridine) (P4VP) NW array was prepared using the PCNP system and used as the template for metallization, because P4VP can effectively adsorb metal nanoparticles and metal ions due to their strong affinity of pyridyl groups.[22,23] P4VP (30 wt %) in dimethlyformamide/ethanol (60:40, w/w) solution is loaded into a nozzle tip (inner diameter 100 μm), and a strong electric field is applied between the tip and a grounded collector. A thin liquid jet is ejected

DOI: 10.1021/acsnano.6b08172
ACS Nano 2017, 11, 3681−3689

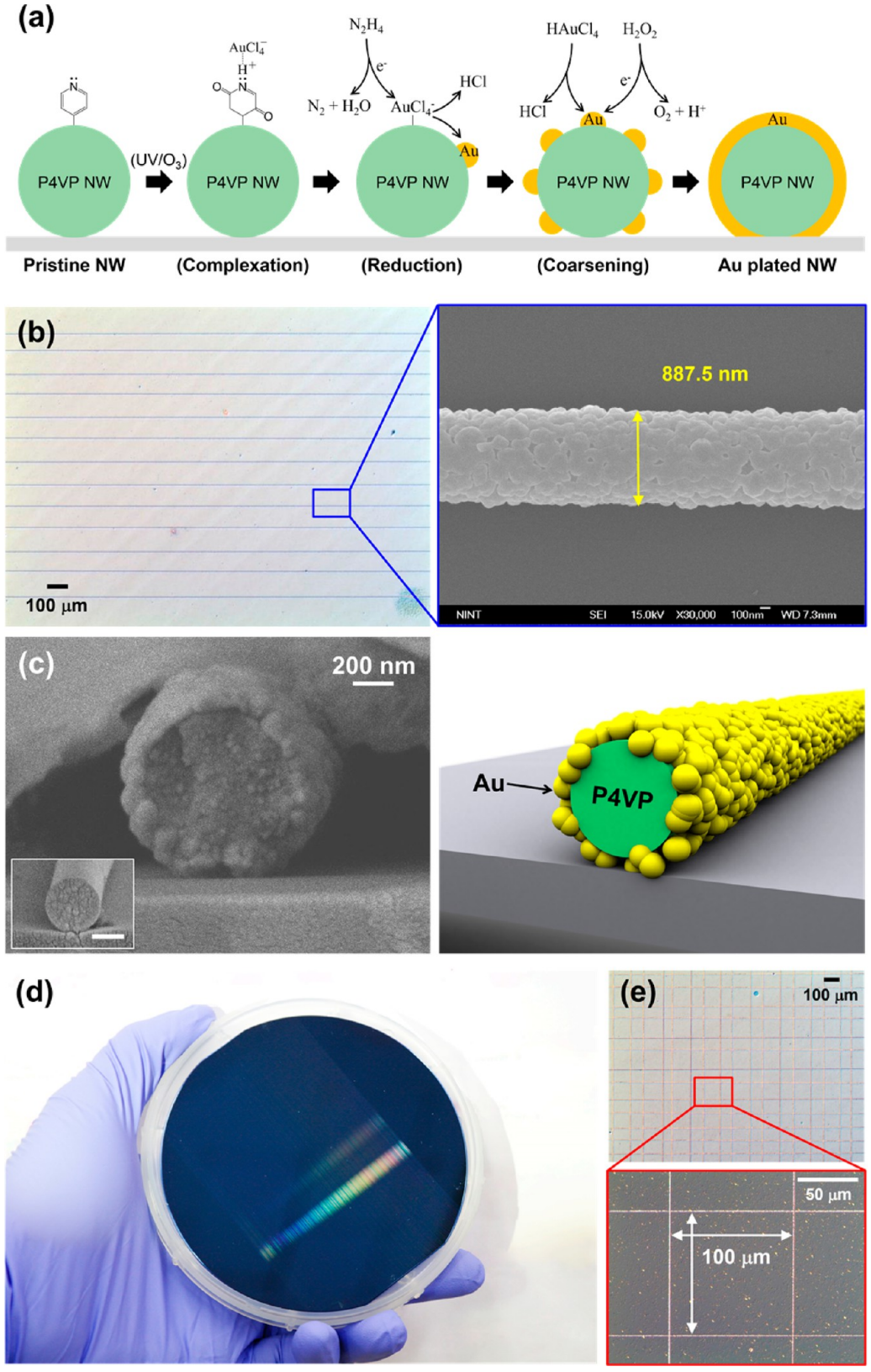

Figure 2. Electroless Au plating on a NW. (a) Schematic diagram of the electroless Au plating procedure on P4VP NW. (b) Parallel pattern of a Au NW array with a 100 μm pitch. (c) Scanning electron microscope (SEM) image (left) and schematic illustration (right) showing a cross-section of an electrolessly plated Au NW (inset: cross-section of a pristine P4VP NW; scale bar, 200 nm). (d, e) Grid pattern of NWs on a 4 in. wafer before (d) and after electroless plating (e).

from the nozzle tip and stretched into a cylindrical NW by electrostatic force. During the flight of the polymer jet, solvent fully evaporates, so a solid polymer NW is deposited on the collector. The tip-to-collector distance is <1 cm, so a stable

DOI: 10.1021/acsnano.6b08172
ACS Nano 2017, 11, 3681−3689

straight jet is maintained until the NW arrives at the collector; this condition is unlike that in conventional electrospinning, in which the jet whips chaotically.[20] The collector is mounted on a motorized $x-y$ stage; maneuvering the stage appropriately during wire formation allows printing of the NW in desired positions and orientations.

Using PCNP, a parallel pattern of P4VP NWs was successfully prepared on a 4 in. Si/SiO_2 (100 nm) wafer and a glass substrate with regular wire spacing of 100 μm and average diameter of 374.8 ± 58.4 nm (Figure 1b, Figure S1). The diameter of printed NWs can be controlled by adjusting the concentration of the solution.[20] PCNP can form a template NW array in various patterns including parallel, wavy, and grid orientations on a large area and is therefore suitable for use as a nanotemplate with a variety of patterns (Figure 1c, Figure S2).

Printed P4VP NWs were oxidized under UV/O_3 (~18.8 mW cm^{-2}, AHTECH LTS Co., LTD) to prevent the dissolution of pristine NWs in solutions that were used in subsequent electroless Au plating processes. Under UV/O_3 treatment, C═C bonds of pyridyl groups in the P4VP are converted by oxygen radicals into carbonyl groups (C═O).[24] Fourier transform infrared (FT-IR) spectroscopy in attenuated total reflection mode verified this conversion (Figure 1d). To obtain a sufficiently intense signal, we prepared the NW mat by collecting P4VP for 10 min on a stationary Al foil substrate. After UV/O_3 treatment for 5 min, the absorbance due to C═C stretching at 1598 cm^{-1} was decreased, and C═O stretching at 1656 cm^{-1} was significantly increased. The pristine NW is soluble in water, whereas the oxidized NW is insoluble and keeps its morphology after water immersion (Figure 1e).

The Au layer was deposited electrolessly on the oxidized P4VP NW array by (i) complexation, (ii) reduction, and (iii) coarsening (Figure 2a). During complexation, Au precursor ions ($AuCl_4^-$) were adsorbed selectively on the pyridyl group of the P4VP NW surface due to the electrostatic interaction between metal-based anions and the protonated pyridyl surface,[22,23] then were reduced to Au nanoclusters or nanoparticles by the vapor of a reducing agent, hydrazine monohydrate ($N_2H_4{\cdot}H_2O$) (Figure S3). The Au nanoparticles provide nucleation sites and act as catalysts for metal plating during subsequent particle enlargement (coarsening), so Au was selectively deposited on the surface of P4VP NWs. Consequently, a Au-plated NW array that had sufficient density to allow electrical percolation was attained (Figure 2b), which was confirmed by the cross-section structure of the NWs: a thin sheath of Au (~100 nm thick) covered a cylindrical P4VP core (Figure 2c). This structure of the polymer core and thin metal sheath has the advantage of high electrical conductivity with high optical transmittance and mechanical bending stability, which will be discussed later. The position and orientation of P4VP template NWs can be precisely controlled by the PCNP; this result suggests that conducting NWs can be obtained in desired patterns and on desired substrates under appropriate conditions for NW printing (Figure 2d,e).

The current–voltage ($I-V$) characteristics of Au NWs aligned between Au pads with a gap of 4 mm demonstrate ohmic contact (Figure 3a, Figure S4a). To calculate the resistivity ρ of the Au NW, we used Ohm's law ($V = IR$), and we assumed that the cross-section of the wire is a perfect circle and only considered the cross-sectional area of the conducting Au shell, which has a cylinder shape excluding the insulating P4VP core. The calculated ρ was 7.5 ± 3.7 $\mu\Omega$ cm, which is only 3.4 times that of bulk Au (2.21 $\mu\Omega$ cm) and 2–3 orders of

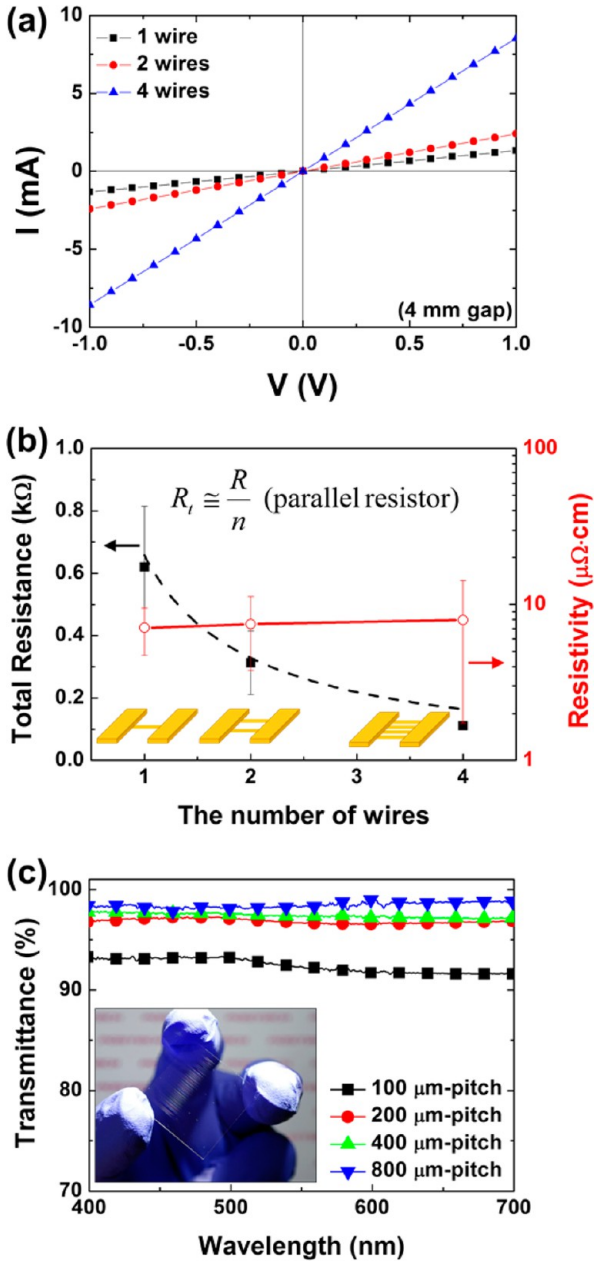

Figure 3. Electrical and optical properties of electrolessly plated Au NWs. (a) Current–voltage ($I-V$) curve and (b) total resistance and resistivity of electrolessly plated Au NWs with different numbers of wires. (c) Optical transmittance of Au NW arrays with different wire spacing (inset: transparent Au NW array with 400 μm pitch).

magnitude lower than previously reported results of electrolessly plated Au NWs.[23,24] The high electrical conductivity of Au NWs can be attributed to the good alignment of the template polymer NWs. Because each P4VP template wire was separated individually without any overlap and hindrance, Au can be deposited on the entire surface of core P4VP NWs. In contrast, previous research works have used a randomly coiled electrospun wire mat as a template.[22,24] So permeation of the metal precursor solution into the wire mat and deposition of the metal layer on the inner surface of the wire mat were hindered by their random geometry, resulting in poor formation of a percolation pathway for electrical transport and poor electrical conductivity. As the number of Au NWs aligned in parallel was increased, the total resistance followed

DOI: 10.1021/acsnano.6b08172
ACS Nano 2017, 11, 3681–3689

the behavior of parallel resistors, and the calculated ρ of wires was nearly unchanged (Figure 3b). Also, the ρ of the wires with different thicknesses of the Au layer showed uniform values of a similar order of magnitude independent of the thickness (Figure S4b). These results mean that all of the Au NWs had uniform electrical characteristics. Previous electrolessly plated conducting NWs have been prepared by electrospinning, so the conducting NWs in the mat were usually randomly coiled and had limited reproducibility of electrical conductivity.[23,25] In contrast, our method can directly produce highly conductive NW arrays with controlled position and orientation without additional thermal treatment or transfer processes; therefore, this method is suitable for various electronic applications based on conducting NWs.

To verify the feasibility of the Au NW array as a transparent electrode, we observed the optical transmittance of parallel-patterned Au NW arrays with different wire spacing. Regardless of the wire spacing, the Au NW array showed a high transmittance of >90% in the entire visible range; the transmittance increased as the wire spacing increased (Figure 3c). This result is attributed to (i) submicrometer wire width, (ii) the highly transparent P4VP core NW (Figure S5), and (iii) the thin Au layer (~100 nm) deposited on the P4VP core (Figure 2c). With high transmittance across the visible range, Au NWs are applicable in transparent electrodes for optoelectronics such as light-emitting diodes, solar cells, and photodiodes.

Our metallic NWs can be directly prepared on a flexible plastic substrate by a room-temperature metallization process, so they can be used as flexible nanoelectrodes. We fabricated a Au NW array on PET substrates (6 and 75 μm thick) and measured resistance changes ($\Delta R/R_0$) after bending with various bending radii (Figure 4a,b). In contrast to the severe resistance change of the ITO film after bending to a radius of <5 mm, the Au NWs did not degrade after bending to a radius of 0.71 mm or after >1000 cycles of repetitive bending to a radius of 3.87 mm (Figure 4b,c). High flexibility and bending stability of the metallic NWs are attributed to the soft polymer NW template and the low dimensionality of Au NWs: the elastic modulus of materials varies with their geometry.[25,26]

A conducting NW array obtained by a low-temperature process is an essential functional unit for transparent and flexible nanoelectronics. Using an individually position-customizable Au NW array, we demonstrated "all-wire transistors", which consist of a poly(3-hexylthiophene) (P3HT) NW channel and Au NW source/drain (S/D) electrodes. To fabricate all-wire transistors, Au NW arrays were prepared with desired wire spacing, which determines channel length. A Au pad (50 nm) was deposited for electrical contact; then PCNP was used to print a semiconducting P3HT NW across the Au NW array (Figure 5a). The resulting device was thermally annealed at 150 °C for 30 min to strengthen the contact between the P3HT NWs and Au NWs. Then a high-capacitance ion-gel film was formed on the P3HT NW and Au NWs as a gate insulator. All-wire transistors on the glass substrate are nearly invisible to the naked eye because of the narrowness of the NW components (Figure 5b). In transfer characteristic (I_D–V_G), all-wire transistors showed high on-current (>10 μA) with low V_D (−1 V) and V_G (−4 V) (Figure 5c). This result is comparable to a device with thermally deposited Au film S/D electrodes.

To calculate hole mobility (μ_h) of the ion-gel gated transistor, we used equations based on the gate-displacement

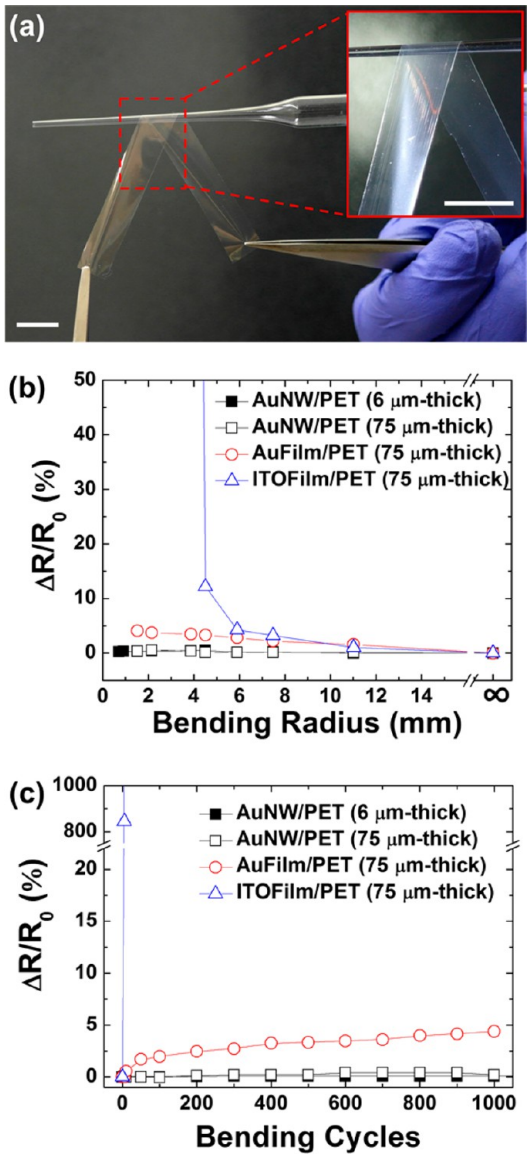

Figure 4. Mechanical bending stability of a flexible Au NW. (a) Photograph of a Au NW array on a 6 μm thick PET substrate. Scale bar: 1 cm. (b, c) Relative resistance changes of a Au NW, Au film, and ITO film on a PET substrate as a function of bending radius (b) and bending cycles with a bending radius of 3.87 mm (c).

current ($I_{Disp} = I_G - I_{Background}$, where I_G is the gate current and $I_{Background}$ is the gate current before turn-on) and induced charge density (P_i):[27,28]

$$P_i = [\int I_{Disp}\, dV_G]/[(dV_G/dt)\, eV] \quad (1)$$

Then

$$\mu_h = \frac{L}{Wd}\frac{I_D}{V_D e P_i} \quad (2)$$

where L is the channel length, W is channel width, d is channel thickness, $e = 1.602 \times 10^{-19}$ C is the elementary charge, and V is channel volume. The all-wire transistor had calculated $\mu_h = 3.5 \pm 1.0$ cm^2 V^{-1} s^{-1} (maximum $\mu_h = 4.7$ cm^2 V^{-1} s^{-1}), which is higher than that of the device based on Au film electrodes (average $\mu_h = 2.0 \pm 0.4$ cm^2 V^{-1} s^{-1}). The excellent electrical characteristics of all-wire transistors are attributed to (i) a larger

DOI: 10.1021/acsnano.6b08172
ACS Nano 2017, 11, 3681−3689

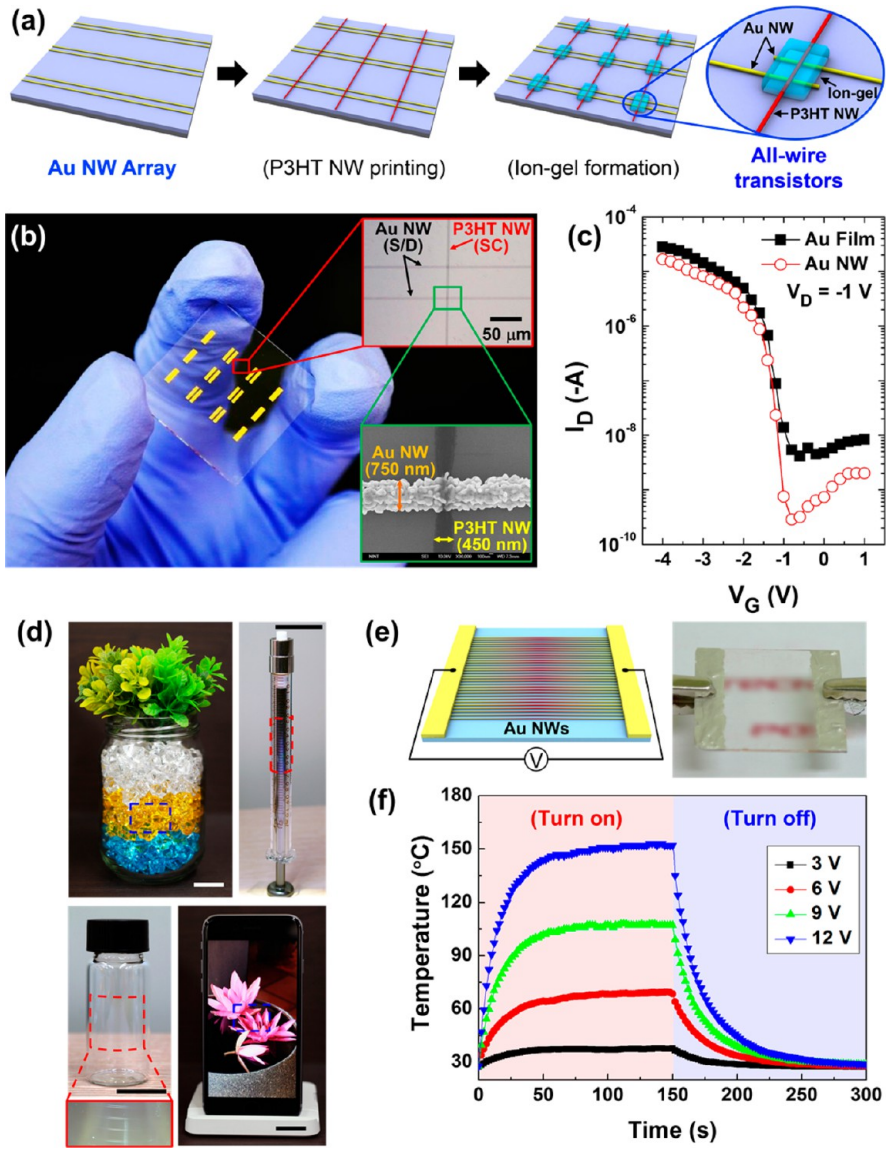

Figure 5. All-nanowire electronics based on a well-aligned Au NW array. (a) Schematic illustrations of the fabrication process for all-wire transistors based on Au NW electrodes and a P3HT NW channel. (b) Transparent all-wire transistor array on a glass substrate (inset: optical microscope (top) and SEM (bottom) images of an all-wire transistor). (c) Transfer characteristics (I_D−V_G) of ion-gel gated P3HT NW transistor based on a Au film (black square) and Au NW (red circle) S/D electrodes. (d) Photographs of the all-wire transistor array transferred on various planar and nonplanar surfaces (a vase, a syringe, a glass vial, and a display of a mobile phone). Scale bar: 2 cm. (e) Schematic illustration (left) and optical image (right) of a transparent Au NW heater. (f) Plot of temperature *versus* time for the NW heater.

induced hole density (~10^{20} cm^{-3}) from high-capacitive ion-gel compared to that from conventional SiO_2-gated devices[29,30] (these holes fill the traps in the channel and smooth the electrical potential variation that is caused by trapped charges)[28] and (ii) extremely low contact resistance (<24.8 Ω cm) in the device (Figure S6). The reduced overlap area between gate insulator and NW S/D electrodes also contributes to the high on/off current ratio in all-wire transistors (Figure S7).

Furthermore, use of position-customizable and room-temperature-processed metallic NWs is not limited by substrates and surfaces, so it can be used to fabricate large-scale transparent and flexible electronic device arrays on various nonplanar surfaces such as vases, glass vials, and syringes (Figure 5d). Therefore, this method provides a promising strategy to develop wire-based advanced electronics for the Internet-of Things and smart healthcare systems.

Furthermore, a transparent Joule heater with a parallel-oriented long Au NW array does not need percolation of NWs; this trait is different from conventional Joule heaters based on short NWs,[31−34] so high-temperature annealing and waste of materials for connection among dispersed NWs are unnecessary (Figure 5e). Ag paste pads were used for electrical contact, and the exothermic properties from the heater were observed using an infrared thermometer. Because the size of Au NWs is too small to adjust a focus of the thermometer on the wires, we measured the temperature of the glass substrate heated by the Au NWs using an emissivity value of the glass (ε = 0.95). The maximum temperature increased with the applied voltage and reached >145 °C at only 12 V (Figure 5f). Effective Joule heating at low input voltage was attributed to the low resistivity

DOI: 10.1021/acsnano.6b08172
ACS Nano 2017, 11, 3681−3689

of Au NWs. Moreover, the heater responded quickly: a constant temperature was reached in <50 s regardless of the applied voltage.

To verify the further potential of the NW heater, a water evaporation test was conducted in air under a controlled relative humidity of 44% and temperature of 25 °C. A 25 μL water droplet on the NW heater evaporated completely within ~151 s at an input voltage of 12 V (Figure S8, Movie S1). Therefore, our NW heater using a highly aligned Au NW array will be useful for applications such automobile window defoggers, which require transparency, high efficiency, and fast response.

CONCLUSION

We developed an easy method that uses ONW templates to prepare position-customizable conducting Au NW arrays without any vacuum or high-temperature processes. Highly aligned Au NWs showed an extremely low resistivity of ~7.5 ± 3.7 μΩ cm (only ~3.4 times higher than that of bulk Au), high optical transmittance (>90%), and stability under mechanical bending; therefore, they enable various electronic applications of Au NWs as nanoelectrodes. Using an Au NW array, we demonstrated transparent all-NW-based electronic applications including transistors and heaters. Because electroless plating techniques have been widely studied to fabricate various kinds of metal layers,[35,36] our method for preparing well-aligned metallic NWs has tremendous scalability. Moreover, our approach to achieve large-area all-wire electronics provides a promising strategy to realize transparent and flexible nanoelectronics and is a breakthrough for practical application of NWs in nanodevices. Further work will involve the development of all-nanowire-based signal input or output devices, which can expand the potential of NW-based future electronics such as transparent and flexible nanoelectronics, textile electronics, and wearable electronics (Figure S9).

EXPERIMENTAL METHODS

Equipment Setup. The position-customizable nanowire printer consists of a syringe pump (NanoNC) mounted vertically over the collector, a gastight syringe (Hamilton), a 32-gauge stainless steel nozzle, a micrometer to control the tip-to-collector distance, a high-voltage generator (NanoNC), and a grounded flat-type collector (20 cm × 20 cm) moved by a linear motor stage (Yaskawa). Another similar PCNP system (Enjet Inc.) was also used.

Fabrication of Aligned P4VP Template Nanowire. To print P4VP NWs with the PCNP system, 30 wt % of P4VP ($M_w \approx 160\,000$, Aldrich) in dimethylformamide (anhydrous, Aldrich)/ethanol (Aldrich) solution (60:40, w/w) was injected through the metal nozzle at 100 nL min^{-1}; the tip-to-collector distance was set at 7 mm and 1.3–1.4 kV was applied to the metal nozzle. While the NW was collected on the substrate, the collector moved in a zigzag at 66.7 cm s^{-1}.

Electroless Au Plating on a Nanowire. Printed P4VP NWs were exposed to UV/O_3 for 5 min. Au precursor ($HAuCl_4 \cdot 3H_2O$, Aldrich) was dissolved in deionized water (0.5 wt %), and the supernatant of the solution was obtained after centrifugation at 18000*g* for 120 min to remove any possible aggregates. Oxidized P4VP NWs were dipped into the Au precursor solution for 30 min, dipped in water to remove excess precursor ions, then blown dry using N_2. Then five drops of diluted hydrazine monohydrate ($N_2H_4 \cdot H_2O$, Aldrich) in water (10%, v/v) were dropped into a Petri dish, and Au precursor adsorbed P4VP NWs were attached to the inside of the Petri-dish cover for 15 min. The specimen was dipped in the water to remove residual N_2H_4 vapor, then blown dry using N_2. Au nanoparticle–P4VP composite NWs were dipped in a solution of $HAuCl_4$, H_2O_2 (30 wt % in H_2O, Aldrich), and deionized water for 5 min. The total volume of the solution was set as 10 mL; 0.2 mL of $HAuCl_4$ (0.5 wt %) and 0.1 mL of H_2O_2 (30 wt %) were used. Water for all experiments was prepared in a Millipore Milli-Q Academic water purification system and had a resistivity of >18.2 MΩ cm.

Device Applications of a Au NW Array. For transistor fabrication, a highly doped silicon wafer and thermally grown SiO_2 (100 nm) or glass were used as substrate. P4VP NWs were printed with various wire spacing and were annealed in ethanol vapor at 55 °C for 10 min to strengthen their adhesion to the substrate. Au NW patterns were prepared using electroless plating. An additional Au layer (50 nm) was thermally deposited as an electrical contact. PCNP was used to print five strands of P3HT NW on the Au NW S/D electrodes, following a previously reported procedure.[20,37] Then the NWs were thermally annealed at 150 °C for 30 min under vacuum to improve the contact between Au NW electrodes and P3HT NWs. For ion-gel gate insulator formation, poly(styrene-*block*-methyl methacrylate-*block*-styrene) (PS-PMMA-PS, synthesized[38]) triblock copolymer, with block molecular masses M_n = 6.2 kg mol^{-1} for PS and M_n = 105 kg mol^{-1} for PMMA, and 1-ethyl-3-methylimidazolium bis-(trifluoromethylsulfonyl)imide ([EMIM][TFSI], Solvent Innovation) ionic liquid were dissolved in ethyl acetate in a 0.7:9.3:90 ratio (w/w) and then drop-cast onto a P3HT NW pattern that had a Au NW S/D contact. The solvent was removed; then an ion-gel film was formed by physical association of the PS blocks in the ionic liquid.

For heater fabrication, a Au NW array with 400 μm wire spacing was prepared on a glass substrate. Ag paste was used to form the electrical contact at both ends of the NWs. The temperature was observed using a thermometer (FLIR T360) with an emissivity of ε = 0.95. For the evaporation test, a 25 μL water droplet was dropped on the Au NW heater, then observed while an input voltage of 12 V was applied.

Characterizations. NW morphology was observed using a scanning electron microscope (Jeol JSM-7401F, National Institute for Nanomaterials Technology, Korea) at an acceleration voltage of 5–15 kV. Optical microscope images were recorded using an optical microscope (Olympus, BX51M). Fourier transform infrared spectroscopy was performed in ATR mode (PerkinElmer, Spectrum Two). The optical transmittance spectra were recorded using a UV–vis spectrophotometer (S-3100, Scinco). All electrical measurements were conducted using a parameter analyzer (Keithley 4200, Keithley Instruments Inc.) in a N_2 atmosphere at room temperature.

ASSOCIATED CONTENT

Supporting Information

The Supporting Information is available free of charge on the ACS Publications website at DOI: 10.1021/acsnano.6b08172.

Diameter distribution of printed pristine P4VP NW array; grid pattern of printed pristine P4VP NW array; SEM images of P4VP NW obtained after complexation, reduction, and coarsening processes; electrical properties of Au NW; transparency of pristine P4VP NW; electrical characteristics of all-wire transistors; evaporation of water droplet on Au NW heater; and schematic illustrations of all-wire electronics (PDF)

Supporting Video S1 (AVI)

AUTHOR INFORMATION

Corresponding Author

*E-mail: twlees@snu.ac.kr; taewlees@gmail.com.

ORCID

Se Hyun Kim: 0000-0001-7818-1903

Cheolmin Park: 0000-0002-6832-0284

Tae-Woo Lee: 0000-0002-6449-6725

Author Contributions

S.-Y.M. conducted most of the experiments including setup of equipment, development of NW metallization technique,

DOI: 10.1021/acsnano.6b08172
ACS Nano 2017, 11, 3681–3689

fabrication of devices, and analysis of data and prepared the manuscript. Y.L. contributed to the fabrication of devices and preparation of the manuscript. S.H.K. contributed to fabrication of devices and analysis of the data. C.P. contributed to analysis of the data and preparation of the manuscript. T.-W.L. initiated the research, designed all experiments, analyzed all data, and prepared the manuscript. All authors discussed the results and contributed to the paper.

Notes

The authors declare no competing financial interest.

ACKNOWLEDGMENTS

This work was supported by the Center for Advanced Soft-Electronics funded by the Ministry of Science, ICT and Future Planning as Global Frontier Project (2013M3A6A5073175), and the Pioneer Research Center Program through the National Research Foundation of Korea funded by the Ministry of Science, ICT & Future Planning (2012-0009460).

REFERENCES

(1) Kim, K. S.; Zhao, Y.; Jang, H.; Lee, S. Y.; Kim, J. M.; Kim, K. S.; Ahn, J.-H.; Kim, P.; Choi, J.-Y.; Hong, B. H. Large-Scale Pattern Growth of Graphene Films for Stretchable Transparent Electrodes. *Nature* **2009**, *457*, 706−710.

(2) Bae, S.; Kim, H.; Lee, Y.; Xu, X.; Park, J.-S.; Zheng, Y.; Balakrishnan, J.; Lei, T.; Ri Kim, H.; Song, Y. I.; Kim, Y.-J.; Kim, K. S.; Özyilmaz, B.; Ahn, J.-H.; Hong, B. H.; Iijima, S. Roll-to-Roll Production of 30-Inch Graphene Films for Transparent Electrodes. *Nat. Nanotechnol.* **2010**, *5*, 574−578.

(3) Wu, Z.; Chen, Z.; Du, X.; Logan, J. M.; Sippel, J.; Nikolou, M.; Kamaras, K.; Reynolds, J. R.; Tanner, D. B.; Hebard, A. F.; Rinzler, A. G. Transparent, Conductive Carbon Nanotube Films. *Science* **2004**, *305*, 1273−1276.

(4) Lipomi, D. J.; Vosgueritchian, M.; Tee, B. C.-K.; Hellstrom, S. L.; Lee, J. A.; Fox, C. H.; Bao, Z. Skin-like Pressure and Strain Sensors Based on Transparent Elastic Films of Carbon Nanotubes. *Nat. Nanotechnol.* **2011**, *6*, 788−792.

(5) Park, J. H.; Lee, D. Y.; Kim, Y.-H.; Kim, J. K.; Lee, J. H.; Park, J. H.; Lee, T.-W.; Cho, J. H. Flexible and Transparent Metallic Grid Electrodes Prepared by Evaporative Assembly. *ACS Appl. Mater. Interfaces* **2014**, *6*, 12380−12387.

(6) Jeong, J.-A.; Kim, H.-K.; Kim, J. Invisible Ag Grid Embedded with ITO Nanoparticle Layer as a Transparent Hybrid Electrode. *Sol. Energy Mater. Sol. Cells* **2014**, *125*, 113−119.

(7) De, S.; Higgins, T. M.; Lyons, P. E.; Doherty, E. M.; Nirmalraj, P. N.; Blau, W. J.; Boland, J. J.; Coleman, J. N. Silver Nanowire Networks as Flexible, Transparent, Conducting Films: Extremely High DC to Optical Conductivity Ratios. *ACS Nano* **2009**, *3*, 1767−1774.

(8) Gaynor, W.; Burkhard, G. F.; McGehee, M. D.; Peumans, P. Smooth Nanowire/Polymer Composite Transparent Electrodes. *Adv. Mater.* **2011**, *23*, 2905−2910.

(9) Kim, J. Y.; Kim, B. H.; Hwang, J. O.; Jeong, S.-J.; Shin, D. O.; Mun, J. H.; Choi, Y. J.; Jin, H. M.; Kim, S. O. Flexible and Transferrable Self-Assembled Nanopatterning on Chemically Modified Graphene. *Adv. Mater.* **2013**, *25*, 1331−1335.

(10) Jeon, H.-J.; Kim, J. Y.; Jung, W.-B.; Jeong, H.-S.; Kim, Y. H.; Shin, D. O.; Jeong, S.-J.; Shin, J.; Kim, S. O.; Jung, H.-T. Complex High-Aspect-Ratio Metal Nanostructures by Secondary Sputtering Combined with Block Copolymer Self-Assembly. *Adv. Mater.* **2016**, *28*, 8439−8445.

(11) Kim, J. Y.; Kim, H.; Kim, B. H.; Chang, T.; Lim, J.; Jin, H. M.; Mun, J. H.; Choi, Y. J.; Chung, K.; Shin, J.; Fan, S.; Kim, S. O. Highly Tunable Refractive Index Visible-Light Metasurface from Block Copolymer Self-Assembly. *Nat. Commun.* **2016**, *7*, 12911.

(12) Kim, J. Y.; Lim, J.; Jin, H. M.; Kim, B. H.; Jeong, S.-J.; Choi, D. S.; Li, D. J.; Kim, S. O. 3D Tailored Crumpling of Block-Copolymer Lithography on Chemically Modified Graphene. *Adv. Mater.* **2016**, *28*, 1591−1596.

(13) Hu, L.; Kim, H. S.; Lee, J.-Y.; Peumans, P.; Cui, Y. Scalable Coating and Properties of Transparent, Flexible, Silver Nanowire Electrodes. *ACS Nano* **2010**, *4*, 2955−2963.

(14) Gong, S.; Schwalb, W.; Wang, Y.; Chen, Y.; Tang, Y.; Si, J.; Shirinzadeh, B.; Cheng, W. A Wearable and Highly Sensitive Pressure Sensor with Ultrathin Gold Nanowires. *Nat. Commun.* **2014**, *5*, 3132.

(15) Wu, H.; Hu, L.; Rowell, M. W.; Kong, D.; Cha, J. J.; McDonough, J. R.; Zhu, J.; Yang, Y.; McGehee, M. D.; Cui, Y. Electrospun Metal Nanofiber Webs as High-Performance Transparent Electrode. *Nano Lett.* **2010**, *10*, 4242−4248.

(16) Wu, H.; Kong, D.; Ruan, Z.; Hsu, P.-C.; Wang, S.; Yu, Z.; Carney, T. J.; Hu, L.; Fan, S.; Cui, Y. A Transparent Electrode Based on a Metal Nanotrough Network. *Nat. Nanotechnol.* **2013**, *8*, 421−425.

(17) Lee, Y.; Kim, T.-S.; Min, S.-Y.; Xu, W.; Jeong, S.-H.; Seo, H.-K.; Lee, T.-W. Individually Position-Addressable Metal-Nanofiber Electrodes for Large-Area Electronics. *Adv. Mater.* **2014**, *26*, 8010−8016.

(18) Xu, W.; Lee, Y.; Min, S.-Y.; Park, C.; Lee, T.-W. Simple, Inexpensive, and Rapid Approach to Fabricate Cross-Shaped Memristors Using an Inorganic-Nanowire-Digital-Alignment Technique and a One-Step Reduction Process. *Adv. Mater.* **2016**, *28*, 527−532.

(19) Lee, Y.; Min, S.-Y.; Kim, T.-S.; Jeong, S.-H.; Won, J. Y.; Kim, H.; Xu, W.; Jeong, J. K.; Lee, T.-W. Versatile Metal Nanowiring Platform for Large-Scale Nano- and Opto-Electronic Devices. *Adv. Mater.* **2016**, *28*, 9109−9116.

(20) Min, S.-Y.; Kim, T.-S.; Kim, B. J.; Cho, H.; Noh, Y.-Y.; Yang, H.; Cho, J. H.; Lee, T.-W. Large-Scale Organic Nanowire Lithography and Electronics. *Nat. Commun.* **2013**, *4*, 1773.

(21) Min, S.-Y.; Kim, Y.-H.; Wolf, C.; Lee, T.-W. Synergistic Effects of Doping and Thermal Treatment on Organic Semiconducting Nanowires. *ACS Appl. Mater. Interfaces* **2015**, *7*, 18909−18914.

(22) Dong, H.; Fey, E.; Gandelman, A.; Jones, W. E. Synthesis and Assembly of Metal Nanoparticles on Electrospun Poly(4-Vinylpyridine) Fibers and Poly(4-Vinylpyridine) Composite Fibers. *Chem. Mater.* **2006**, *18*, 2008−2011.

(23) Park, S.; Moon, S. C.; Chen, D.; Farris, R. J.; Russell, T. P. Preparation of 1 Inch Gold Nanowires from PS-B-P4VP Block Copolymers. *J. Mater. Chem.* **2010**, *20*, 1198−1202.

(24) Park, M.; Im, J.; Park, J.; Jeong, U. Micropatterned Stretchable Circuit and Strain Sensor Fabricated by Lithography on an Electrospun Nanofiber Mat. *ACS Appl. Mater. Interfaces* **2013**, *5*, 8766−8771.

(25) Hsu, P.-C.; Kong, D.; Wang, S.; Wang, H.; Welch, A. J.; Wu, H.; Cui, Y. Electrolessly Deposited Electrospun Metal Nanowire Transparent Electrodes. *J. Am. Chem. Soc.* **2014**, *136*, 10593−10596.

(26) Fedorchenko, A. I.; Wang, A.-B.; Cheng, H. H. Thickness Dependence of Nanofilm Elastic Modulus. *Appl. Phys. Lett.* **2009**, *94*, 152111.

(27) Xia, Y.; Cho, J. H.; Lee, J.; Ruden, P. P.; Frisbie, C. D. Comparison of the Mobility-Carrier Density Relation in Polymer and Single-Crystal Organic Transistors Employing Vacuum and Liquid Gate Dielectrics. *Adv. Mater.* **2009**, *21*, 2174−2179.

(28) Xia, Y.; Cho, J. H.; Paulsen, B.; Frisbie, C. D.; Renn, M. J. Correlation of on-State Conductance with Referenced Electrochemical Potential in Ion Gel Gated Polymer Transistors. *Appl. Phys. Lett.* **2009**, *94*, 13304.

(29) Wang, G.; Swensen, J.; Moses, D.; Heeger, A. J. Increased Mobility from Regioregular poly(3-Hexylthiophene) Field-Effect Transistors. *J. Appl. Phys.* **2003**, *93*, 6137−6141.

(30) Scheinert, S.; Paasch, G. Interdependence of Contact Properties and Field- and Density-Dependent Mobility in Organic Field-Effect Transistors. *J. Appl. Phys.* **2009**, *105*, 14509.

(31) Jin, C. Y.; Li, Z.; Williams, R. S.; Lee, K.-C.; Park, I. Localized Temperature and Chemical Reaction Control in Nanoscale Space by Nanowire Array. *Nano Lett.* **2011**, *11*, 4818−4825.

(32) Jin, C. Y.; Yun, J.; Kim, J.; Yang, D.; Kim, D. H.; Ahn, J. H.; Lee, K.-C.; Park, I. Highly Integrated Synthesis of Heterogeneous

DOI: 10.1021/acsnano.6b08172
ACS Nano 2017, 11, 3681−3689

Nanostructures on Nanowire Heater Array. *Nanoscale* **2014**, *6*, 14428−14432.
(33) Kim, D.; Zhu, L.; Jeong, D.-J.; Chun, K.; Bang, Y.-Y.; Kim, S.-R.; Kim, J.-H.; Oh, S.-K. Transparent Flexible Heater Based on Hybrid of Carbon Nanotubes and Silver Nanowires. *Carbon* **2013**, *63*, 530−536.
(34) Kim, T.; Kim, Y. W.; Lee, H. S.; Kim, H.; Yang, W. S.; Suh, K. S. Uniformly Interconnected Silver-Nanowire Networks for Transparent Film Heaters. *Adv. Funct. Mater.* **2013**, *23*, 1250−1255.
(35) Mallory, G. O.; Hajdu, J. B. *Electroless Plating: Fundamentals and Applications*; William Andrew, 1990.
(36) Zhu, J.; Jiang, W. Fabrication of Conductive Metallized Nanostructures from Self-Assembled Amphiphilic Triblock Copolymer Templates: Nanospheres, Nanowires, Nanorings. *Mater. Chem. Phys.* **2007**, *101*, 56−62.
(37) Hwang, S. K.; Min, S.-Y.; Bae, I.; Cho, S. M.; Kim, K. L.; Lee, T.-W.; Park, C. Non-Volatile Ferroelectric Memory with Position-Addressable Polymer Semiconducting Nanowire. *Small* **2014**, *10*, 1976−1984.
(38) Hadjichristidis, N.; Pispas, S.; Floudas, G. *Block Copolymers: Synthetic Strategies, Physical Properties, and Applications*; John Wiley and Sons, 2003.

DOI: 10.1021/acsnano.6b08172
ACS Nano 2017, 11, 3681−3689